Influence of thermal and water treatment on strength recovery for soda lime silica glass

Kyriaki Corinna Datsiou [a], Telesilla Bristogianni [b], Fred Veer [b], Christian Louter [c], Mauro Overend [b]

a. Centre for Engineering Research, School of Physics, Engineering and Computer Science, University of Hertfordshire, Hatfield, Hertfordshire AL10 9AB, United Kingdom, k.c.datsiou@herts.ac.uk
b. Department of Architectural Engineering & Technology, Faculty of Architecture & the Built Environment, TU Delft, Julianalaan 134, 2628 BL Delft, The Netherlands.
c. Department of Materials, Mechanics, Management & Design, Faculty of Civil Engineering & Geosciences, TU Delft, Stevinweg 1, 2628 CN, Delft, The Netherlands.

Abstract

Glass is highly sensitive to damage accumulation during its service life, leading to a significant reduction in strength. Annealed glass used in glazing units of low-rise buildings can experience a 71-85% strength reduction after 20-30 years of natural weathering, which can be detrimental in structural applications. Despite these considerable reductions in strength, there are currently no well-established methods for repairing glass components, with hypothetical repair methods primarily limited to resin injection and little evidence on their durability or their efficiency in preventing water diffusion and subcritical crack growth. As glass panels increase in size, complexity and cost, the standard approach of replacing damaged components with new glass becomes unsustainable. This paper develops effective and durable thermal healing methods for damaged glass components. A systematic experimental investigation is undertaken involving controlled artificial aging of annealed glass, followed by thermal healing, microscopy and destructive flexural tests to assess the effectiveness of the repairs. Different thermal and hydrothermal profiles are explored showing that thermal treatment has potential for strength recovery. In fact, thermal healing for the flaws in this study, at high temperatures in the order of 300-500°C, can fully restore and even increase the design strength of glass beyond new as-received strength. This suggests that thermal healing can support and promote repair and reuse of end-of-life glass, enhancing circularity in the architectural glass industry.

Keywords

glass, flaws, scratch, repair, thermal treatment, water soaking, healing, strength recovery

Article Information (this info will be completed later by the editors)

- Published by GPD, on behalf of the author(s)
- Published as part of the peer-reviewed Glass Performance Days Conference Proceedings, June 2025
- Editors: Jan Belis, Christian Louter & Marko Mökkönen

1. Introduction

Its transparent nature makes glass a highly desirable material for vision and display panels in the architectural, automotive, and marine industries. Over recent decades, glass applications have increased, with larger glazed surface areas becoming distinctive features of the built environment, enabled by technological advances in glass processing. While this trend aligns with end-user demands for increased transparency, it also contributes to a growing volume of post-consumer glass. In Europe alone, glass waste generated from building renovations in 2013 reached 1.3Mt (Hestin et al., 2016). This is expected to increase in the coming years due to ongoing efforts to upgrade the existing low energy-performance building stock to meet the UK's Net Zero policy (HM Government, 2021) and European energy policies (European Commission, 2020) among other national and international climate actions.

Even though glass is theoretically infinitely recyclable, the post-consumer circularity of architectural glass remains limited in practice (Hartwell et al., 2023). Glass manufacturing is currently one of the most energy intensive industries (Hutton et al., 2021), however, current manufacturing and replacement practices focus on new glass, contributing to increased glass waste that largely ends up in low grade aggregate or landfill (Hartwell et al., 2023). To date only a small percentage of recovered glass follows a truly circular model. This is limited to glass offcuts from the manufacturing and post-processing stages, due to the absence of high purity cullet arising from construction and demolition (C&D) waste. At present, glass from C&D waste streams is at best downcycled, finding use as aggregate in cementitious or asphalt matrices (Mohajerani et al., 2017) or in secondary applications such as the glass wool, glass packaging and glass bead industries (Hestin et al., 2016). While reuse offers improved environmental benefits to recycling (European Commission, 2016), its practical application remains in its infancy. Recent studies in architectural glass, emphasized the potential for glass reuse after disassembly (Cupać et al., 2024; Rota et al., 2023; Teich et al., 2024) and highlighted its associated environmental benefits (Reshamvala et al., 2024), however, practical challenges currently prevent wide adoption in industry.

In addition to challenges related to insulated glazing unit (IGU) disassembly, non-destructive evaluation and persuading designers to specify- and clients to accept- post-consumer glass, its mechanical degradation over time remains a critical point of attention. Annealed glass used in glazing units of low-rise buildings and exposed to 20-30 years of natural weathering, suffered a 71-85% reduction in strength at low probabilities of failure (Cupać et al., 2024; Datsiou & Overend, 2017; Overend & Louter, 2015). The extent of strength reduction is governed by surface flaws, that act as stress concentration points under crack-opening actions. Surface flaws accumulate during transportation, installation and in-service conditions, including scratches from cleaning, accidental damage and pits due to impact from wind-borne debris. As a result, their typology, size, density and distribution vary depending on service life duration, orientation, location, and level of exposure (Rota et al., 2023). The decline in strength together with absence of standardised quality assessment protocols, introduce several uncertainties that could discourage designers from specifying post-consumer glass in practical applications.

Despite the proven environmental benefits of glass reuse and the significant strength degradation in post-consumer glass, there is lack of well-established methods for restoring its mechanical performance. Current repair methods for glass involve resin application, either through direct injection in a surface flaw (Koob, 2000; Overend & Louter, 2015) or in the form of a coating (Hand et al., 2003; Laouamri et al., 2016), to volumetrically fill visible surface flaws. Resin injection resulted in improved strength of damaged glass components, with acrylic outperforming epoxy resins (Overend & Louter, 2015). Additionally, acrylic coatings applied to sandblasted glass were found to improve optical quality by restoring light transmission to 90% (Laouamri et al., 2016). However, the durability of resin repair or the extents to which they penetrate the deepest flaw parts and prevent water diffusion and subcritical crack growth are not well documented.

Thermal treatment has emerged as a promising method for repairing surface flaws in glass by facilitating morphological changes at the crack interface. For temperatures near or exceeding the glass transition point, cracks undergo transformation such as blunting and pinching at the crack tip, rounding of radial cracks and receding of lateral and median cracks (Blaeß & Müller, 2023; Hrma et al., 1988). These effects are primarily driven by material viscous flow, making temperature a key factor in thermal healing. Simultaneous exposure to increased temperature in combination with water vapour pressure was found to further expedite crack healing for surface and subsurface damage (Wang et al., 2020, 2021a; Wilson & Case, 1999). This is attributed to the reaction between the fractured Si-O bonds at the crack interface and the available water molecules, forming silanol groups. Silanol groups decrease the glass viscosity locally and enhance material viscous flow and thus morphological changes at the crack interface (Girard et al., 2011; Wang et al., 2021b). Similar effects were observed in abraded silica glass, where heat treatment at 1200°C under wet conditions significantly improved surface roughness compared to dry conditions (Osawa et al., 2011).

While the existing literature mainly focuses on detection of morphological crack changes under thermal treatment, strength recovery investigation has been also undertaken. Zaccaria & Overend (2015) investigated the potential of thermal treatment (560°C for 2 hours) for repairing realistic (Griffith) flaws in glass with various edge treatments. Their findings however were not conclusive, demonstrating a 35% increase in strength for polished-edge glass at low fractile values but a strength decrease for as-cut and ground-edge glass. This potentially suggests that crack healing may be only possible for small flaws such as the ones found in polished-edge glass. Similarly, Schwind et al. (2020) reported a 12% and 41% increase in mean surface strength in artificially aged soda lime silica glass, treated at 300°C and 500°C respectively. However, their sample size was small and insufficient for producing statistically meaningful conclusions.

The aim of this paper is to further investigate the potential of thermal treatment as a repair solution for surface strength recovery of end-of-life post-consumer glass or damaged glass components, with ultimate goal of extending service life and promoting reuse. This is achieved through flexural destructive strength characterisation of artificially scratched soda lime silica annealed glass. Prior to testing, controlled damage is introduced in the glass samples, which are then either left untreated or subjected to heat treatment, with or without prior water soaking. Details on the materials, sample preparation and the experimental procedure are described in Section 2. The flexural strength data are then statistically analysed, and results from different treatments are compared to the untreated and as-received series to determine strength recovery at low probabilities of failure, which are relevant for engineering design. Additionally, digital microscopy is used to capture typical scratch patterns before and after treatment, providing visual insights into the effect of the repair process. Results and their discussion are available in Section 3 while salient conclusions are summarised in Section 4.

2. Materials and Methods

2.1. Glass specimens

As-received, annealed, soda lime silica glass has been used throughout in this study. All glass samples originated from a single 4mm thick glass sheet that was cut in pieces of 160x160 mm^2 with a water jet cutter. No edge treatment was applied, with edge quality remaining in as-cut form. Five series of glass, each comprising 20 samples, were used in this study resulting in a total of 100 samples, one series for each of untreated and as-received glass and three for artificially aged, treated glass. An overview of the series and the treatment scenarios are presented in Table 1. The number of samples per series was selected to allow statistical analysis and interpretation of glass strength data, following recommendations in Datsiou (2017) for a minimum number of 15 samples per series. During sample preparation, a UV-light detector was used to distinguish the tin side of the glass. For consistency, atmospheric side (commonly known as the “air” side, i.e. the side exposed to the H_2/N_2 environment during the float process) was tested for all series.

Table 1: Glass series overview.

Series	Abbr.	Sample No.	Condition	Treatment
As-received	AR	20	As-received	Untreated
Scratched	SC	20	Scratched (16N)	Untreated
Heat Treated 1	HT300	20	Scratched (16N)	Treated (3hrs / 300ºC)
Heat Treated 2	HT500	20	Scratched (16N)	Treated (3hrs / 500ºC)
Water soaked & Heat Treated	WHT500	20	Scratched (16N)	Treated (46hrs / RH100% & 3hrs / 500ºC)

2.2. Artificial ageing

The scratching device (Fig. 1a) used in Datsiou & Overend (2016) was used to produce a single, controlled surface scratch on each sample from the scratched series in Table 1. The device featured a 90º tungsten carbide tip with a radius of 120μm (Fig. 1b), attached to a platform loaded with a mass of 1.0kg, resulting in a total weight of 1.6kg on the scratching tip (indenter). The device was manually moved in a sliding action across the glass surface, guided by a straight-edged steel plate, to produce a linear scratch of 10mm length at the centre of each specimen. The indenter produced scratches (Fig. 1c) with varying width, falling within the micro-ductile (~135μm wide) and in some cases the microcracking regimes (~ 240μm wide) (Schneider et al., 2012).

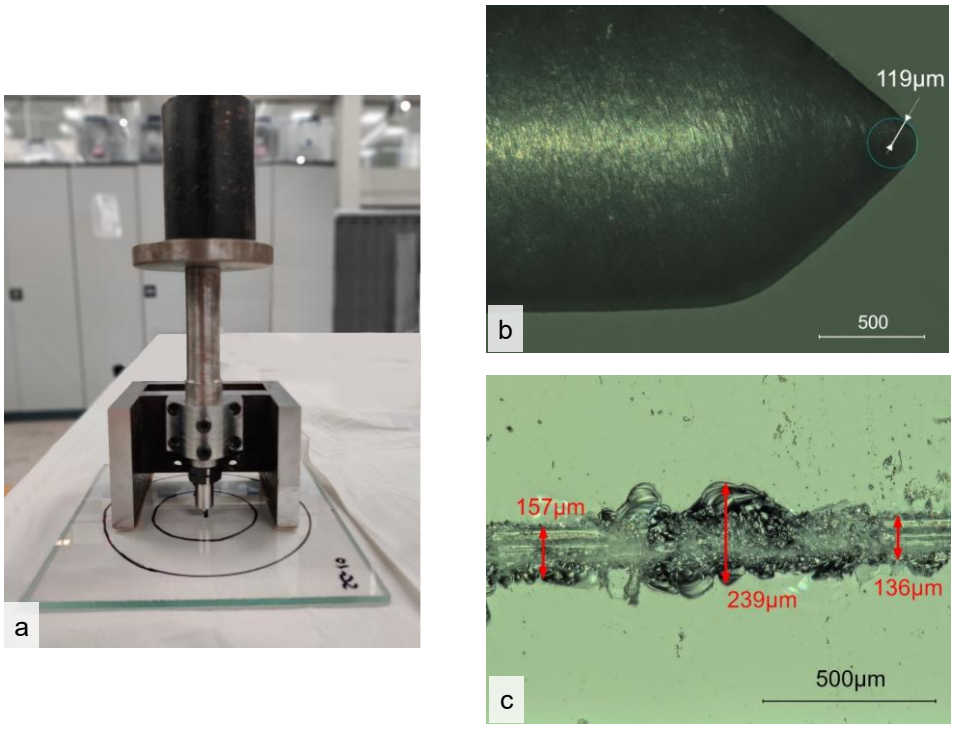

Fig. 1: Artificial ageing: (a) Scratching device; (b) indenter tip and (c) typical induced scratch.

2.3. Hydrothermal and thermal treatment

Following artificial ageing at ambient conditions, the series HT300 and HT500 were subjected to heat treatment in a convection furnace (ROHDE ELS 1000S, Germany) at temperatures of 300 and 500ºC, respectively, for 3 hours. The heating rate was performed at 47-48ºC/hr while the cooling rate was 40ºC/hr to minimise risk of thermal shock in the glass (thermal treatment profiles available in Fig. 2b). The samples were placed flat on the refractory fibre board (Ceraboard ®) positioned at the base of the furnace chamber, with the artificially aged surface facing upwards to ensure uniform heat exposure

and prevent introduction of additional flaws from contact with the furnace surface (Fig. 2a). The maximum temperature for heat treatment of 500°C was selected just below the transition temperature of soda lime silica glass (typically ~550°C), ensuring the material remains within the solid region. Additionally, the 300°C treatment scenario was selected to investigate the potential of energy-saving solutions, aligning with sustainability considerations.

Prior to thermal treatment, series WHT500 was water soaked for a total of 46hrs in a stainless-steel water bath used in Louter et al., (2012) (Fig. 3). The bath was filled with tap water (14.6°C) and was gradually heated to a temperature of 70°C, at a heating rate of 2.6°C/hr. After 42 hrs the heating element was switched off and at 46hrs the water was drained, allowing the samples to cool down naturally to room temperature. Water soaking at elevated temperature was undertaken to enhance water adsorption, which can modify surface chemistry, and locally lower the viscosity at the crack tip. Water molecules react with the silicon oxygen network of the glass surface, breaking the siloxane bonds and forming silanol groups (Eq. 1), which can weaken the glass network and promote surface diffusion (Doremus, 1995). The hydrated surface leads to a decrease in surface viscosity, that can in turn facilitate viscous flow and thermal healing.

$$Si\text{-}O\text{-}Si + H_20 \rightarrow Si\text{-}OH + HO\text{-}Si \qquad \text{Eq. 1}$$

Directly after water soaking, the WHT500 samples were heat treated at 500°C following an identical treatment profile as HT500 (Fig. 2b) This enables a direct comparison between the thermal response of “water soaked” and “dry” samples, providing information on the influence of adsorbed water during heat treatment.

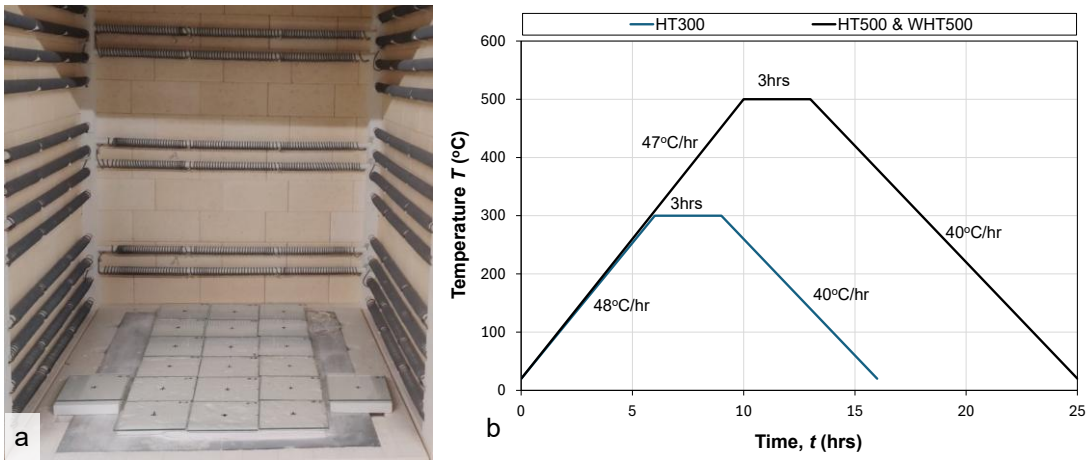

Fig. 2: Thermal treatment of artificially aged glass: (a) glass furnace and; (b) programmed thermal treatment profiles.

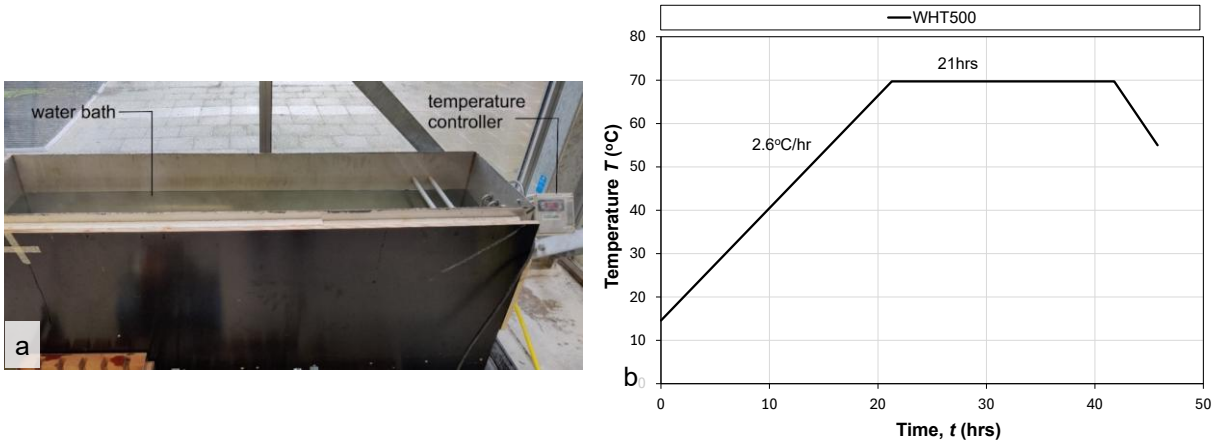

Fig. 3 Water soaking treatment: (a) water tank and (b) recorded water temperature profile.

2.4. Performance evaluation

The performance of the thermal and hydrothermal repair was evaluated using qualitative non-destructive and quantitative destructive techniques described below.

Surface characterisation: Surface characterisation was undertaken through digital microscopy (Keyence VHX-7000, Japan, Fig. 4) for representative samples in two stages: (a) after artificial ageing and; (b) following thermal / hydrothermal treatment to observe any visual improvement in scratch morphology as a result of the treatment.

Flexural strength characterisation: The flexural strength of the samples was subsequently evaluated by destructive testing in a coaxial double ring set-up (Fig. 4). The dimensions of the loading and the support rings were 60mm and 120mm respectively, in accordance with ASTM C1499-08 (2009). A Unitronic 50kN Universal Testing Machine was used to apply a vertical load up to glass fracture, at a stress rate of 25MPa/s. This rate was selected to trigger rapid fracture and minimise subcritical crack growth during the test. The “air” side of the specimen, i.e. the surface where artificial aging and repair (if applicable to the series) had been performed, was subjected to tension during the test. A clear self-adhesive film was applied on the tin / compressive side prior to the test to retain fragments after fracture and assess whether fracture occurred within or outside the loading ring.

The failure load was converted to failure stress following ASTM C1499-08 (2009). To further mitigate any influence of subcritical crack growth, the failure stress results were converted to a 60-sec equivalent strength. The tests data were subsequently statistically analysed and fitted in a two-parameter Weibull distribution (Eq. 2) following the methodology in Datsiou & Overend (2018). This approach allowed the determination of strength at specific probabilities of failure, P_f. In this study, strength values at mean, P_f=50%, and low probabilities of failure, P_f=8‰ in accordance with ASTM E1300-16 (2016) and typically used in engineering design, are discussed. Hazen’s estimator was used to assign cumulative probabilities of failure to the collected data, as it provides accurate and conservative strength estimates for small sample sizes at low probabilities of failure (Datsiou & Overend, 2018).

$$P_f = 1 - e^{\left[\left(-\frac{\sigma_{f,60}}{\theta}\right)^{\beta}\right]} \qquad \text{Eq. 2}$$

where P_f is the probability of failure, $\sigma_{f,60}$: the 60s-equivalent stress, β: the shape factor and θ: the scale factor of the Weibull distribution.

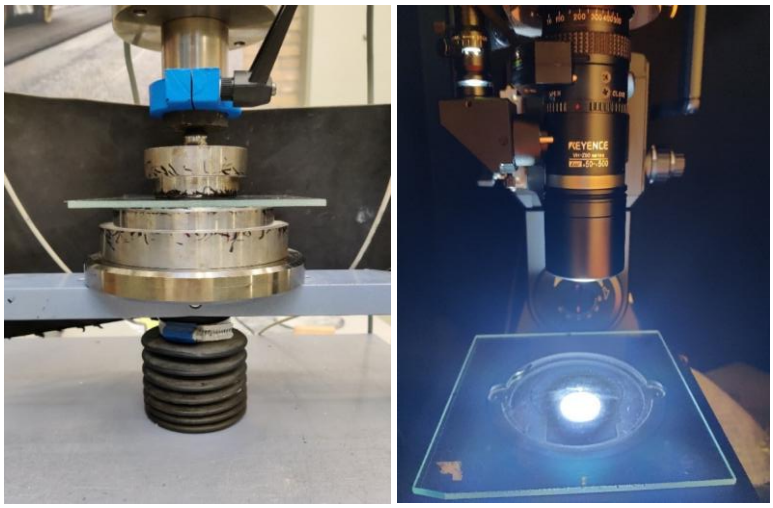

Fig. 4: Coaxial double ring set-up (left) and; digital microscopy (right).

3. Results & Discussion

3.1. Scratch morphological changes

Digital microscopy revealed that surface damage is fairly consistent across different samples within the same series (Fig. 5). However, surface damage varies across different series depending on the selected treatment scenario.

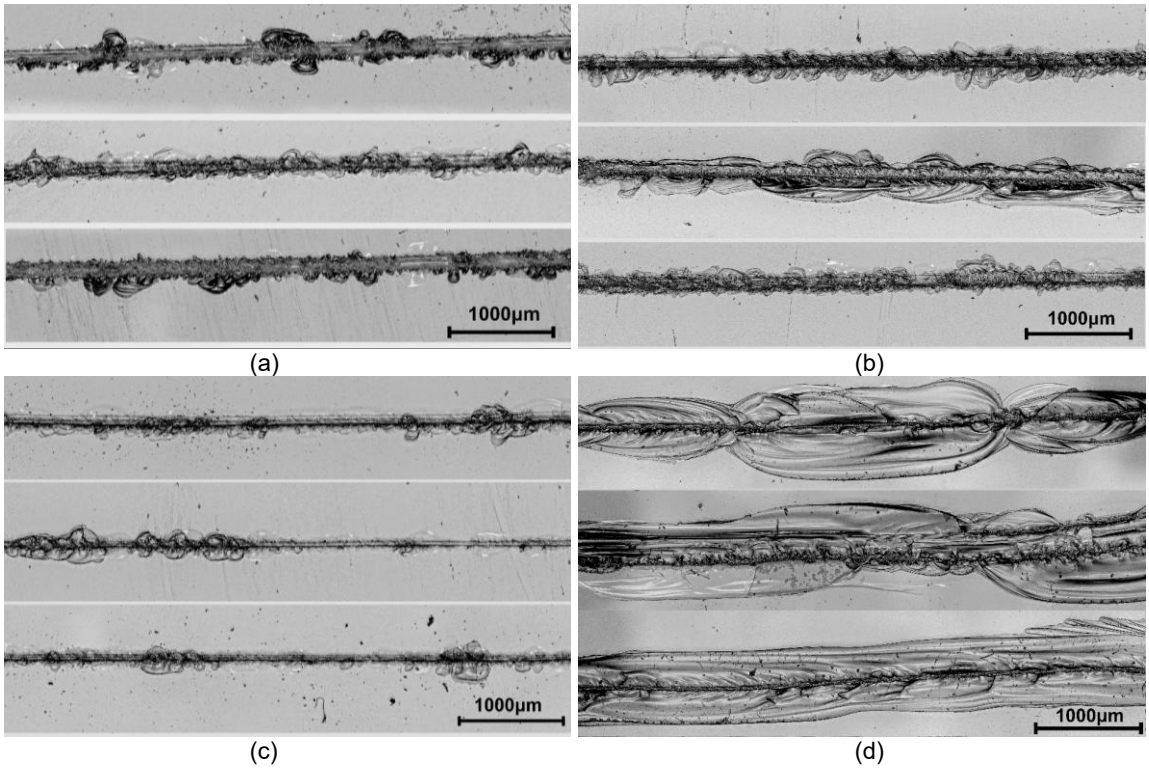

Fig. 5: Micrographs for 3 representative samples from each of the: (a) SC; (b) HT300; (c) HT500 and; (d) WHT500 series.

As discussed previously, the scratched and unrepaired samples (SC), featured scratches that belonged to the micro-ductile and micro-cracking regime, depending on the location across the scratch length (Fig. 5a). The micro-ductile regime is associated with scratches without radial cracks or significant lateral cracks, whereas the micro-cracking regime involves scratches where lateral cracks are apparent and intersect with the surface (Schneider et al., 2012).

Scratches in HT300 samples (Fig. 5b) have similar features to the SC series, except for a very slight rounding of the crack edges, that may indicate a degree of softening. This suggests that 300ºC is not sufficient for any significant morphological changes to take place along the scratch length for the given treatment duration. Noticeable improvement is however, observed for the HT500 samples (Fig. 5c). Although scratches have not disappeared, it is evident that the width of the scratch is smaller. This indicates that, despite being below the transition temperature of glass, heat treatment at 500ºC, can facilitate viscous flow and partially trigger thermal healing.

Finally, the most significant morphological change is observed for the WHT500 series (Fig. 5d). However, instead of improving scratch appearance, the hydrothermal treatment had the opposite effect, causing significant deformation of the scratches, with bubble-like features forming around the scratch length. This suggests that any lateral cracks formed beneath the surface during artificial ageing, extended to the surface during the water treatment. This may be attributed to subcritical crack growth, triggered by the presence of water and residual stresses that were locally introduced during the scratch

indentation. Additionally, despite the subsequent thermal treatment at 500°C, the water accentuated damage could not be reverted, indicating that the effectiveness of thermal treatment is highly dependent on the extent of pre-existing damage.

3.2. Flexural strength

An overview of the Weibull cumulative distribution functions (CDFs) for all series is presented in Table 2. The results indicate that all series exhibit an acceptable Anderson Darling goodness of fit, p_{AD}, except for WHT500, which falls below the selected significance level (p_{AD}<0.05). This implies that WHT500 does not fit to a Weibull distribution, potentially due to the varying extent of subcritical crack growth induced by water soaking, which altered the scratch morphology sufficiently so that the series can no longer be represented by one flaw population.

Table 2: Weibull CDF summary table.

Series	Failure stress range		Weibull parameters and goodness of fit				Fractile values	
	maxσ (MPa)	minσ (MPa)	Shape factor β	Scale factor θ	p_{AD}	CV %	$\sigma_{0.008}$ (MPa)	$\sigma_{0.5}$ (MPa)
AR	108.9	60.4	5.6	87.3	0.206	20.7	36.9	81.8
SC	53.3	41.8	10.3	47.7	0.051	11.7	29.8	46.0
HT300	58.1	46.3	14.0	54.1	0.754	8.7	38.4	52.7
HT500	72.6	60.4	13.1	67.1	0.819	9.3	46.4	65.2
WHT500	60.9	49.1	10.3	54.2	0.008	11.7	33.9	52.3

Unsurprisingly, the highest strength at mean probabilities of failure (P_f=50%), was observed in the as-received (AR) series (Fig. 6a). Similarly, the scratched and unrepaired (SC) series exhibited the lowest strength, with a respective reduction of 19% and 44% at low (P_f=0.008) and mean probabilities of failure compared to the AR series (Fig. 6a). The variation in strength reduction is linked to the shape factor, β, of the Weibull distribution, which dictates the slope of the linear CDF. A lower shape factor in AR results in a CFD with a smaller slope, leading to lower strength at low probabilities of failure which also indicates greater variability in failure stress data. This is attributed to the diverse flaw sizes present on the surface of as-received glass. On the contrary, the scratched series were artificially aged following an identical protocol that ensured relatively controlled and repeatable scratches, with low data variability, resulting in a coefficient of variation, CV, of only 12%, compared to 21% for AR glass.

More importantly, thermal treatment for dry samples was found to be effective for strength recovery, with 500°C (HT500) outperforming 300°C (HT300) (Fig. 6b). Even though significantly below the transition temperature of glass, treatment at 300°C resulted in a 29% and 77% strength improvement compared to the SC series, at P_f=0.008 and P_f=0.5 probabilities of failure, respectively. These percentages increased to 56% and 119% for the HT500 series. In fact, thermal treatment at both 300°C and 500°C for 3hrs, fully restored the strength of glass at low probabilities of failure, even exceeding the strength of AR glass by 4% and 26%, respectively (Table 2). Although this does not apply for mean probabilities of failure, with HT300 and HT500 reaching only 64% and 80% of the strength of AR glass, respectively. HT300 and HT500 also exhibit very similar shape factors, β, resulting in almost parallel CDFs, which potentially indicates a linear shift of the CFD as a function of temperature, although further testing is required to reliably establish this relationship.

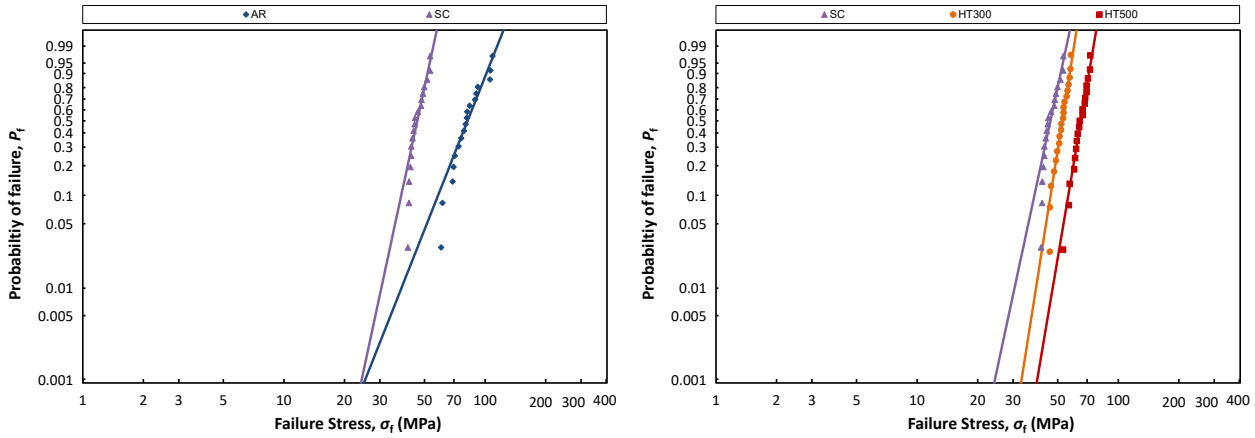

Fig. 6: Cumulative distribution function for series: (a) as-received (AR) and scratched and unrepaired (SC) and; (b) scratched and unrepaired (SC), heat treated at 300°C (HT300) and heat treated at 500°C (HT500).

The series subjected to water soaking followed by heat treatment (WHT500) also resulted in strength recovery, albeit partial, compared to the scratched and unrepaired series (SC) with respective 34% and 52% strength improvements at P_f=0.008 and P_f=0.5. However, even though an identical thermal treatment profile (including maximum treatment temperature and duration) has been used for repairing the HT500 and WHT500 samples, the strength recovery in "water-soaked" samples was found to be inferior to "dry" samples (Fig. 7a). This implies that the morphological changes observed in WHT500 samples (lateral cracks extending to the glass surface, Fig. 5d) outweighed any potential viscosity-lowering benefit as a result of the water adsorption during water soaking. Additionally, the strength improvement for WHT500 closely matched HT300 at mean probabilities, with HT300 outperforming WHT500 at low probabilities of failure, despite its higher treatment temperature (Fig. 7b).

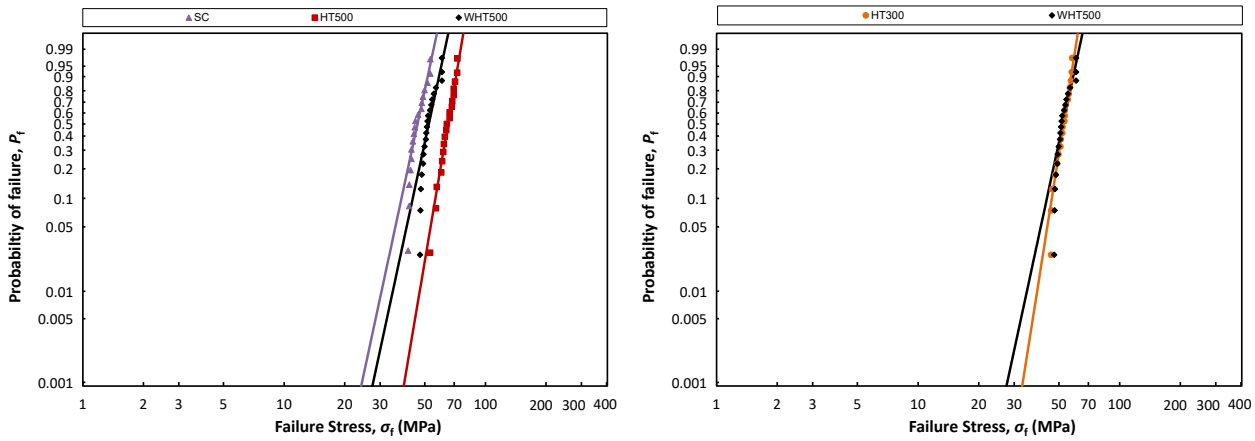

Fig. 7: Cumulative distribution function for series: (a) scratched and unrepaired (SC), heat treated at 500°C (HT500) and water soaked and heat treated at 500°C (WHT500) and; (b) Heat treated at 300°C (HT500) and water soaked and heat treated at 500°C (WHT500).

3.3. Potential of thermal healing and practical limitations

While direct application of thermal healing on naturally aged glass is yet to be undertaken to date, heat treatment of artificially scratched glass in this study showed promising potential for improving the mechanical performance of aged glass in real-world applications. Heat treatment at 300 and 500°C was particularly effective, restoring strength to levels comparable to- or even exceeding- as-received strength at low probabilities of failures. Notably, the 300°C treatment fully restored the design strength of glass to higher levels than as-received glass, indicating that 300°C would suffice for the flaws

investigated in this study, in engineering applications where low fractile values govern design. This suggests that thermal treatment has the potential to be integrated into industrial processes for extending the lifespan of damaged or end-of-life glass components, reducing material waste and supporting repair and reuse. However, it must be acknowledged that practical limitations exist. This process cannot be implemented on site and requires large scale industrial furnaces for treating full scale components. While heat treatment at 300°C was found to be less effective overall than 500°C, the trade-off between repair effectiveness and energy efficiency must be considered.

Additionally, although strength improvement is evident, the investigated thermal treatments were not able to fully restore the optical quality of the artificially scratched glass. Scratches were still visible after treatment, limiting practical application of reused treated panels in high-end architectural applications where optical quality is essential, whilst the presence of these defects could still act as trigger locations for subcritical crack growth during the service life of the glass. Understanding these limitations is crucial for further optimisation and ultimately translating thermal healing into a reliable industry practice.

4. Conclusions

This study investigated the potential of thermal treatment for repairing artificially scratched, soda lime silica glass, focusing on its effectiveness in both thermal healing and strength recovery. The experimental method involved artificial ageing to produce a single and controlled scratch on the surface of each sample and investigated with qualitative non-destructive and quantitative destructive tests the potential of different thermal repair scenarios, including one preceded by water soaking.

The findings show that thermal treatment can improve glass strength, with treatment temperature being a crucial factor in strength recovery and the morphology improvement achieved. Treatment at both 300°C and 500°C, not only fully restored glass strength but also exceeded the strength of as-received glass at low probabilities of failure. However, water soaking prior to heat treatment, which was initially assumed to lower viscosity locally and facilitate crack healing through viscous flow, instead promoted subcritical crack growth triggered by the presence of water molecules at the crack tip and the influence of residual stresses, potentially induced by the scratch indentation. This limited the strength recovery of water-soaked samples compared to the equivalent dry heat treatment, indicating that any beneficial reduction in viscosity was outweighed by deleterious subcritical crack growth. Although visual improvement was not observed for scratched glass treated at 300°C, microscopy demonstrated that treatment at 500°C significantly improved the scratch morphology, reducing the width of the scratch. However, the extent of morphological improvement depended on the initial scratch severity, as the extensive damage caused by subcritical crack growth in the water-soaked glass could not be improved with the same treatment.

To fully develop the potential of thermal healing, further research is required to evaluate its effectiveness in repairing flaws of varying severity and typology (e.g. pits). Exploring alternative process parameters, such as exposure to water vapor during thermal treatment or increasing the treatment temperature closer to the transition temperature of glass could further enhance thermal healing, improving viscous flow. Additionally, to support technology uptake, it is essential to assess the applicability of thermal healing on naturally aged, post-consumer glass, demonstrating feasibility for real-world scenarios. Beyond engineering performance, future studies should also quantify the economic and environmental benefits to determine its viability as a large-scale sustainable repair solution for glass components.

Acknowledgements

Funding from the Royal Society for the research grant “ReStruct Glass: Repair methods for structural glass” for the University of Hertfordshire is gratefully acknowledged. The authors would also like to

thank Bas Vahl and Hens van Ginhoven at TU Delft for providing technical support.

References

ASTM C1499-08. (2009). Standard Test Method for Monotonic Equibiaxial Flexural Strength of Advanced Ceramics at Ambient Temperature. *ASTM International*.

ASTM E1300-16. (2016). Standard Practice for Determining Load Resistance of Glass in Buildings. *ASTM International*.

Blaeß, C., & Müller, R. (2023). Viscous healing of Vickers indentation–induced cracks in glass. *Journal of the American Ceramic Society*, *106*(10), 5795–5805. https://doi.org/10.1111/jace.19245

Cupać, J., Datsiou, K. C., & Louter, C. (2024). Reuse potential of architectural glass: experimental study on the strength of used window glazing. *Glass Structures and Engineering*. https://doi.org/10.1007/s40940-024-00267-y

Datsiou, K. (2017). Design and Performance of Cold Bent Glass. *PhD Thesis, University of Cambridge*.

Datsiou, K. C., & Overend, M. (2016). Evaluation of Artificial Ageing Methods for Glass. *Challenging Glass 5 Conference*, 581–591.

Datsiou, K. C., & Overend, M. (2017). Artificial ageing of glass with sand abrasion. *Construction and Building Materials*, *142*, 536–551. https://doi.org/https://doi.org/10.1016/j.conbuildmat.2017.03.094

Datsiou, K. C., & Overend, M. (2018). Weibull parameter estimation and goodness-of-fit for glass strength data. *Structural Safety*, *73*, 29–41. https://doi.org/https://doi.org/10.1016/j.strusafe.2018.02.002

Doremus, R. H. (1995). Diffusion of water in silica glass. *Journal of Materials Research*, *10*(9), 2379–2389. https://doi.org/10.1557/JMR.1995.2379

European Commission. (2016). *EU Construction & Demolition Waste Management Protocol*.

European Commission. (2020). *A Renovation Wave for Europe - greening our buildings, creating jobs, improving lives*. https://eur-lex.europa.eu/legal-content/EN/TXT/?uri=CELEX%3A52020DC0662

Girard, R., Faivre, A., & Despetis, F. (2011). Influence of water on crack self-healing in soda-lime silicate glass. *Journal of the American Ceramic Society*, *94*(8), 2402–2407. https://doi.org/10.1111/j.1551-2916.2011.04517.x

Hand, R. J., Ellis, B., Whittle, B. R., & Wang, F. H. (2003). Epoxy based coatings on glass: strengthening mechanisms. *Journal of Non-Crystalline Solids*, *315*, 276–287. www.elsevier.com/locate/jnoncrysol

Hartwell, R., Coult, G., & Overend, M. (2023). Mapping the flat glass value-chain: a material flow analysis and energy balance of UK production. *Glass Structures and Engineering*, *8*(2), 167–192. https://doi.org/10.1007/s40940-022-00195-9

Hestin, M., De Veron, S., & Burgos, S. (2016). *Economic study on recycling of building glass in Europe*.

HM Government. (2021). *Net Zero Strategy: Build Back Greener*.

Hrma, P., Han, W. T., & Cooper, A. R. (1988). Thermal healing of cracks in glass. *Journal of Non-Crystalline Solids*, *102*, 88–94.

Hutton, G., Clark, H., Bolton, P., & Carver, D. (2021). *Energy intensive industries*.

Koob, S. P. (2000). New techniques for the repair and restoration of ancient glass. *Studies in Conservation*, *45*(sup 1), 92–95. https://doi.org/10.1179/sic.2000.45.supplement-1.92

Laouamri, H., Giljean, S., Arnold, G., Kolli, M., Bouaouadja, N., & Tuilier, M. H. (2016). Roughness influence on the optical properties and scratch behavior of acrylic coating deposited on sandblasted glass. *Progress in Organic Coatings*, *101*, 400–406. https://doi.org/10.1016/j.porgcoat.2016.09.014

Louter, C., Belis, J., Veer, F., & Lebet, J. P. (2012). Durability of SG-laminated reinforced glass beams: Effects of temperature, thermal cycling, humidity and load-duration. *Construction and Building Materials*, *27*(1), 280–292. https://doi.org/10.1016/j.conbuildmat.2011.07.046

Mohajerani, A., Vajna, J., Cheung, T. H. H., Kurmus, H., Arulrajah, A., & Horpibulsuk, S. (2017). Practical recycling applications of crushed waste glass in construction materials: A review. In *Construction and Building Materials* (Vol. 156, pp. 443–467). Elsevier Ltd. https://doi.org/10.1016/j.conbuildmat.2017.09.005

Osawa, K., Inoue, H., Masuno, A., Katayama, K., Zhang, Y., Utsuno, F., Sugahara, Y., Koya, K., Fujinoki, A., Tawarayama, H., & Kawazoe, H. (2011). Smoothing of surface of silica glass by heat treatment in wet atmosphere. *Journal of Applied Physics*, *109*(103520). https://doi.org/10.1063/1.3587229

Overend, M., & Louter, C. (2015). The effectiveness of resin-based repairs on the inert strength recovery of glass. *Construction and Building Materials*, *85*, 165–174. https://doi.org/https://doi.org/10.1016/j.conbuildmat.2015.03.072

Reshamvala, M., Rauh, K., Kießlich, P., Ayvaz, I., Länge, J., Elstner, M., Pfanner, D., & Schuster, M. (2024). Case Study on the Re-use Potential of Insulated Glass Units. *Challenging Glass 9 Conference Proceedings*, *9*. https://doi.org/10.47982/cgc.9.638

Rota, A., Zaccaria, M., & Fiorito, F. (2023). Towards a quality protocol for enabling the reuse of post-consumer flat glass. *Glass Structures and Engineering*, *8*(2), 235–254. https://doi.org/10.1007/s40940-023-00233-0

Schneider, J., Schula, S., & Weinhold, W. P. (2012). Characterisation of the scratch resistance of annealed and tempered architectural glass. *Thin Solid Films*, *520*(12), 4190–4198.

Schwind, G., von Blücher, F., Drass, M., & Schneider, J. (2020). Double ring bending tests on heat pretreated soda–lime silicate glass. *Glass Structures and Engineering*, *5*(3), 429–443. https://doi.org/10.1007/s40940-020-00129-3

Teich, M., Scherer, C., Schuster, M., Brandenstein, M., & Elstner, M. (2024). Reuse and remanufacturing of insulated glass units. *Glass Structures and Engineering*, *9*, 339356. https://doi.org/10.1007/s40940-024-00276-x

Wang, C., Wang, H., Gao, R., Zhang, M., Liu, S., Hou, J., & Chen, X. (2021a). Experimental investigation on thermal healing of subsurface damage in borosilicate glass. *Ceramics International*, *47*(12), 17128–17138. https://doi.org/10.1016/j.ceramint.2021.03.022

Wang, C., Wang, H., Gao, R., Zhang, M., Liu, S., Hou, J., & Chen, X. (2021b). Experimental investigation on thermal healing of subsurface damage in borosilicate glass. *Ceramics International*, *47*(12), 17128–17138. https://doi.org/10.1016/j.ceramint.2021.03.022

Wang, C., Wang, H., Liu, Z., Zhang, M., Gao, R., Hou, J., & Chen, X. (2020). Kinetic model and effect of surface impurities on the crack healing of BK7 glass. *Ceramics International*, *46*(11), 19069–19077. https://doi.org/10.1016/j.ceramint.2020.04.239

Wilson, B. A., & Case, E. D. (1999). Effect of humidity on crack healing in glass from in-situ investigations using an ESEM. *Journal of Materials Science*, *34*, 247250. https://doi.org/https://doi.org/10.1023/A:1004484901369

Zaccaria, M., & Overend, M. (2015). Thermal Healing of Realistic Flaws in Glass. *Journal of Materials in Civil Engineering*, *04015127*, 1–9.